

DESIGN OF NANOMATERIALS TOWARD THE CONTRAST ENHANCEMENT IN MAMMOGRAPHY IMAGES FOR BREAST CANCER DIAGNOSIS

Y. M. Hernández-Rodríguez, A. Ashok, Oscar E. Cigarroa-Mayorga*

Dept. Advanced Technologies, UPIITA-Instituto Politécnico Nacional, Av. IPN
No. 2580, C.P. 07340, México

ocigarroam@ipn.mx

Hernández-Rodríguez, Y. M., Ashok, A., & Mayorga-Cigarroa, O. E. (2023). Design of nanomaterials toward the contrast enhancement in mammography images for breast cancer diagnosis. In E. San Martín-Martínez (Ed.). *Research advances in nanosciences, micro and nanotechnologies. Volume IV* (pp. 53-72). Barcelona, Spain: Omniascience.

Abstract

In this chapter, the characteristics of several materials for application in medical imaging are discussed. This text is focused on breast cancer, and thus, it is mentioned in deep since the effects on human health until the medical tools to give a medical diagnosis. A complete panorama of breast cancer is offered to the reader in the introduction section. Thus, the chapter starts with the meaning of cancer and the statistics of this disease. Then, the mammography images are mentioned as the current techniques for the diagnosis, particularly the use of X-ray beams and the physics involved in the image generation. Afterward, experimental results about Mn-oxide based nanoparticles are shown. The synthesis of nanoparticles was performed through accessible methods of synthesis from chlorides compounds. And then, the nanoparticles were functionalized with silicon oxide for enhancing the biocompatibility of the material. The physical properties of nanoparticles were studied by X-ray diffraction, scanning electron microscopy, transmission electron microscopy, energy dispersive X-ray spectroscopy, Raman spectroscopy, and X-ray photoelectron spectroscopy. Artificial breast tissue was obtained to test the nanoparticles and studied the behaviour in the tissue. The possibility of employing the nanoparticles as contrast enhancement material for breast cancer diagnosis is discussed.

Keywords: breast cancer, accessible methods of synthesis, nanoparticles, early diagnosis, hydrothermal, artificial breast tissue.

1. Introduction

Cancer is a complex disease where a group of cells in the human body tend to grow out of control. It is known that one of the most common cancer-associated death among women is the breast cancer in the world. Invasive ductal carcinoma and invasive lobular carcinoma are the two main kinds of cancer found in the breast of women. These cancer cells begin in ducts and lobules parts of the breast, respectively [1]. A variety of factors, mainly genetic, aging, and environmental factors, are associated with the initiation and progression of breast cancer. The new cases of breast cancer patients have been rising day by day. However, the death rate through breast cancer is reduced by 43 % during 1990-2020 due to the development of various types of therapies for the early detection and monitoring of patients [2]. Generally, breast cancer is diagnosed using various techniques, namely breast ultrasound, diagnostic mammogram, imaging techniques, biopsy, etc. The imaging techniques are suitable for the detection of early breast cancer stages, which include mammography, positron emission tomography (PET), magnetic resonance imaging (MRI), computed tomography (CT) scan, and single-photon emission computed tomography (SPECT) scan, ultrasound, and X-rays, among others. These imaging technologies constitute a tool for determining the type and stage of breast cancer by the creation of visual representations from the mama and the medical interpretation of these medical analyses. Among these imaging techniques, the mammography technique has been attractive for the detection of cancers at an early stage of development that can reduce the risk of dying due to breast cancer disease. The mammography imaging technique utilizes a low-dose X-ray system as a source for visualizing the tissue inside the breasts [3]. It contains several advantages (i.e., high sensitivity and specificity, inexpensive, well tolerated, etc.) for diagnosis and monitoring of patients in the early stages of cancer. Besides these various benefits, mammography imaging is limited by technical performance, quality of practices, and the patient-centered way of working. It has been shown from previous studies that the utilization of external substances or materials or nanomaterials will be needed for developing emerging opportunities.

Breast cancer detection is categorized into three distinct stages: identification of an abnormality in the breast tissue by an imaging technique (usually mammography), diagnosis of cancer using imaging modalities plus a biopsy assay, and characterization of abnormalities to determine a prognosis and an appropriate course of treatment [4 – 6]. Mammography is designed for detecting breast cancer

using radiographic examination. The performance of mammography imaging has been improving for several decades by developing advanced detector technologies and powerful computers [7, 8]. Recently, digital mammography is used for the early detection of breast cancer, which offers the promise of revolutionizing mammography imaging and effective screening through its superior dose, diagnostic accuracy, and control performance. The physical principles of mammography are connected with breast composition, radiation energy, X-ray spectra, compression, scattered radiation control, and magnification [9]. Breast tissue is composed of milk glands, ducts and lobules, fatty tissues, and supportive tissues. Depending on the compositions of these components, breast tissue is divided into dense breast tissue and non-dense breast tissue. Mammography is helpful to detect early breast cancer by determining the ratio of non-dense tissue and dense tissue. Mammography uses X-rays to get images from breast tissue, which has a modest impact on contrast. The shape of the X-ray spectrum in mammography is dependent on the energy of applied potential and target/filter combination [9, 10]. Higher X-ray energies can provide lower doses or better image quality even for patients with dense breasts. The energies of X-rays used in mammography are generally found in the range of 22-49 keV. Therefore, finding the optimum X-ray spectrum provides valuable information about image quality and dose efficiency. Breast compression is another important parameter in mammography imaging techniques. For effective early breast cancer detection, the amount of exposed breast tissue should be increased. Breast compression reduces radiation or improves image quality by lowering scatter radiation, geometric blurring, and anatomical super-position [2, 9]. After interacting X-rays with the breast tissues, the radiation will be scattered in various directions. More scattered radiation produces by denser and thicker glandular tissue than by the thinner, fatty, and transparent tissues. To get high-contrast imaging, lower amounts of scattered radiation are preferred. The grid generally consists of strips of lead, which are used to reduce undesired scattered radiation that damages the image quality. The performance of image quality is related to the grid ratio (i.e., the ratio of strip height to strip spacing). The greater grid ratio is suitable to achieve the high efficiency of the grid and required radiation dose [9]. The increment of image quality is performed by reducing breast thickness and air-gap technique. The imaging radiation then reaches the image receptor system that consists of a single intensifying screen with a luminescent coating and a special single-emulsion film. The film must be exposed to the proper film-screen system and radiation quality to visualize the diagnosis in the optimum range. Afterward, film processing is required for changing the image contrast, fog, noise, and sensitivity. Solid-state detectors are utilized to record the scattered radiation that converts

the scattered radiation into electronic signals. These electronic signals are sent to a computer for displaying images on the monitor. The analysis of image quality can visualize the characteristic morphology of a mass, the shape and spatial configuration of calcifications, distortion of the normal architecture of the breast tissue, the asymmetry between images of the left and right breasts, development of anatomically definable new densities [10]. The quantitative and qualitative descriptions of image quality are influenced by the nature of the X-ray spectrum, X-ray absorption properties at the anatomic region, geometric sharpness, the resolution characteristic curve, noise properties of the imaging system, etc. The complete process of the mammography imaging technique is presented in Figure 1. All the parameters used in mammography should be optimized properly to achieve effective resolution of the image so that it will be useful for detecting cancer present in the breast.

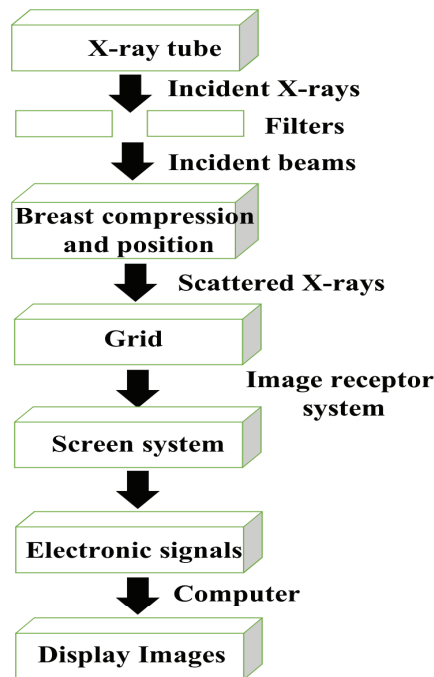


Figure 1. Components of mammographic imaging techniques.

Nowadays, the development of new testing devices as well as materials has been improved for facilitating the detection of cancer. Nanotechnology is a growing field of research, which involves the understanding and control of matter at the nanometer scale [11]. Nanotechnology offers new opportunities for the

reduction of cost, working time, as well as environmental pollution. Nanocarriers used for cancer diagnosis and therapeutic cancer drugs are divided mainly into organic and inorganic, which are made from lipids, polymers, proteins nucleic acid, metals, carbon, micelles, liposomes, dendrimers, and nanoparticles [12, 13]. The development of these nanoparticles is dependent on various factors, such as the shape and size of the particle, surface chemistry, composition, potential, elasticity, etc. Many of the applications of nanotechnology utilize nanomaterials for designing devices and systems due to their unique physical as well as chemical properties. Nanomaterials are characterized by unique physicochemical properties, such as small feature size in the range of 1-100 nanometers, large surface area to mass ratio, and high reactivity that can be metals, ceramics, biomaterials, polymeric materials, or composite materials. These properties of nanomaterials make them different from bulk materials in general design processes and their objectives. Based on dimensions, nanomaterials are divided into four different classes: zero-dimensional nanomaterials (i.e., quantum dots, fullerenes, and nanoparticles, etc.), one-dimensional nanomaterials (i.e., nanotubes, nanofibers, nanorods, nanowires, and nanohorns, etc.), two-dimensional nanomaterials (i.e., nanosheets, nanofilms, and nanolayers, etc.), three-dimensional nanomaterials (i.e., bulk powders, dispersions of nanoparticles, arrays of nanowires and nanotubes, etc.) [3, 13]. The variety of nanomaterials and their new properties have been applied from extraordinarily tiny electronic devices to biomedical devices. Nanomaterials can serve as vehicles for the delivery of therapeutic agents, detectors, or guardians against early disease and perhaps repair of metabolic or genetic defects. Various types of nanomaterials, namely nanoparticles (i.e., Ag, Au, SiO₂, TiO₂, Fe₂O₃, etc.), quantum dots, carbon structures (i.e., graphene, graphene oxide), dendrimers, and nanogels (i.e., polypeptides, collagen) have been using since several decades for medical imaging. With growing advances in mammography imaging, several nanomaterials using different nanoparticles of gold, silver, platinum, aluminum, palladium, copper, iron, silica, gold-coated Fe₃O₄, gold-silver alloy, silver sulfide, silica encapsulated silver, etc. have been employed by various research groups [11 – 16]. Nanomaterials are also used as imaging agents. The use of these nanomaterials in early cancer detection and therapy is promising to overcome the limitations found in the conventional diagnosis methods and identification of abnormalities.

There are several examples of nanomaterials that have been used to enhance the detection and diagnosis of cancers, namely quantum dots, carbon-based nanomaterials (carbon nanotubes, buckyballs, nanodiamond), metal- or oxide-based nanomaterials (gold, silver, aluminum, magnetic iron oxide, titanium

dioxide, zinc oxide, silica, etc.), liposomes, and polymer-based nanomaterials (polysaccharides, polypeptides, polyelectrolytes, dendrimers, and polynucleotides). These nanomaterials have desirable characteristics that facilitate their use for screening and imaging. These nanomaterials contain unique characteristic properties, namely small size and shape in nanoscale, large surface area to mass ratio, increased fraction of atoms at the surface, chemical compositions, multifunctional capabilities, and high reactivity. The mechanical properties (i.e., strength, brittleness, hardness, toughness, fatigue strength, plasticity, elasticity, ductility, rigidity, yield stress, etc.), thermal properties (thermal conductivity, thermoelectric power, heat capacity, and thermal stability, etc.), magnetic properties (diamagnetic, paramagnetic, ferromagnetic, antiferromagnetic, ferrimagnetic, etc.), electrical, optical, and catalytic properties are the most important physicochemical properties of nanomaterials [13, 17, 18]. The understating of nanotechnology, cancer biology, immunomedicine, and nanoparticle surface chemistry has provided a better clue to prepare the effective immuno-nanomedicine for cancer therapy. Moreover, the selection of nanoparticles type and its composition is essential for development of efficient drug delivery system (DDS). These properties are mainly dependent on the size and shape of nanomaterials, which are different from bulk materials of the same composition. For improving the contrast in mammography imaging, various properties of nanomaterials have been studied thoroughly. The nanomaterials should have the properties, such as small size and shape, high X-ray absorbance, low cytotoxicity, high permeability and retention, chemically inert, high adaptability, strong near-infrared absorber, ability to alter electromagnetism properties, easily controlled features, high stability, good tolerability, etc. for contrast enhancement [3, 18] including in ultrasonography, computed tomography, scintigraphy, and magnetic resonance imaging. Nanoparticles have become more prevalent in reports of novel contrast agents, especially for molecular imaging and detecting cellular processes. Fluorescent nanoparticles can easily be tuned for specific imaging purposes. They offer a more intense fluorescent light emission, longer fluorescence lifetimes, and a much broader spectrum of colors than conventional fluorophores. Nanoparticle contrast agents for ultrasound have also been developed, which may enhance the sensitive detection of vascular and cardiac thrombi, as well as solid tumors of the colon, liver, and breast, in a noninvasive manner. Most common materials that have been used for the development of photo-based nanoparticles (NPs). To enhance the quality of imaging compared with the conventional technique, various techniques, namely a combination of nanomaterials with a superconducting quantum interface device, metal alloys, a

combination of metal nanoparticles with semiconductors, magnetic nanoclusters, etc. are also employed. With these recent developments for enhancing contrast, nanomaterials could improve the chances of locating tumors, and tracking their levels and microcalcifications in the breast tissue with high selectivity, special resolution, and sensitivity for early detection [12]. Although these nanomaterials are promising in the field of medical imaging, the use of nanomaterials is limited by their cost, time, safety, and complexity. Various types of nanomaterials, such as thin films, multilayers, nanotubes, nanofilaments, nanometer-sized particles, etc. have been synthesized by many different techniques. The choice of the particular synthesis techniques for nanomaterials depends on diverse features such as source materials, nature of substrate, required film thickness, specific application of nanomaterials, material's purity, material's stability, repeatability, uniformity, flexibility, etc. These features are directly related to the material properties and production costs. Depending on the quality of synthesized nanomaterials and fabrication cost, techniques for the synthesis of nanomaterials are generally divided into two categories: physical-based and chemical-based techniques. The physical-based methods like thermal evaporation, sputtering, molecular beam epitaxy, pulsed laser deposition, etc., are normally designed to synthesize high-quality materials with fewer impurities, showing more reliable and reproducible techniques. Electrochemical processes, chemical polymerization, sol-gel, chemical vapor deposition, colloidal dispersion, hydrothermal route, etc., are some examples of chemical-based techniques for the synthesis of nanomaterials. Solution-based techniques possess cost-effective devices due to their simplicity of the deposition process, ease to handle, require less energy usage, better material utilization, and use of potentially low energetic incentives (i.e., low substrate temperatures, atmospheric environment, etc.). The completed information about these methods and their respective advantages, disadvantages, and types of nanomaterials to be synthesized is found in the reported literature [1, 19, 20]. The synthesis of nanomaterials is a complex process, which can be categorized into various steps: generation of the atoms/molecules from the source, transport of the source atoms/molecules to the substrate (or container), nucleation process, and growth of nanomaterials. At present, the synthesis techniques play a vital role in controlling the structures of nanomaterials at the nanoscale. The optical, electrical, magnetic, biological, structural, and morphological properties of nanomaterials can be tailored depending on the synthesis techniques and synthesis parameters. Based on these properties, nanomaterials can be used in a variety of applications. Image processing is a vital step in the quantification of structural features from images. Morphology is another

technique of image processing, which is based on the shape and form of objects. Generally, morphology utilizes a structuring element to an input image for creating an output image of the same size. Morphological operations such as erosion, dilation, opening, and closing are used to perform morphological image analysis [21]. The Breast Imaging-Reporting and Data System classified mammographic features into various categories of morphology, namely punctuated (round or oval shape), amorphous (rounding or flaking shaped), coarse heterogeneous (irregular and conspicuous), fine pleomorphic (more conspicuous), and fine linear and fine linear branching (thin, irregular linear) [22]. These morphologies are mainly dependent on the size and shape of images. The formation of an image of an object or breast cancer tissue involves different steps, such as capturing the image, digitization, transmission, etc. The technique adopted for enhancing the quality of an image is also called contrast enhancement. Numerous contrast enhancement methods, namely, histogram stretching or histogram equalization technique, algorithms, thresholding, classical image filtering, wavelet transformation, mathematical morphology techniques, multifractal models, etc., have been proposed to improve the contrast of images [21 – 26]. All these techniques are designed to improve the contrast of images by analyzing multicomponent images, removing the noise in high frequency, increasing the distribution of gray levels, analyzing the quantitative description of complex structures, minimizing the homogeneity of co-occurrence matrix of the original image, sharpening medical images, removing the clouds to achieve more clarity, among others. Recently, techniques based on mathematical morphology are applied for contrast enhancement due to their advantages over other techniques for providing better visualization of images. Mathematical morphology uses mathematical principles and relationships to extract the components of images, which are based on the structural properties of objects [23, 24]. It uses an input image and processing operator for image processing that involves selective extraction of the features followed by contrast enhancement.

2. Experimental procedure

Two materials were explored: (1) Mn_3O_4 , and (2) MnFe_2O_4 nanoparticles. To synthesize the Mn_3O_4 nanoparticles, manganese (II) chloride, deionized water with 18 M Ω as resistivity value, two inches epi ready silicon wafers (1 0 0) were commercially acquired from MERK (SIGMA-ALDRICH). On the other hand, to obtain the MnFe_2O_4 nanoparticles, iron chloride, and manganese chloride

were used as metal sources, and sodium dodecyl sulfate, ethanol, and sodium hydroxide, were commercially obtained from the same provider. The functionalization of nanoparticles with silicon oxide was performed by using ammonia, and tetraethyl orthosilicate, which were commercially obtained. In addition, artificial breast tissue was made based on our previous work [27] to evaluate the behavior of synthesized materials. Thus, xylene, benzalkonium chloride, ammonium hydroxide, alumina, hydrogen peroxide, acetone, glycerin, agar, silicon carbide, and methanol were commercially acquired from MERK (SIGMA-ALDRICH). All the reagents were used without further purification process.

To raise the Mn_3O_4 nanoparticles the known spray pyrolysis methodology was employed according to our previously reported methodology [28]. Thus, the manganese chloride was used to prepare a 0.5 M aqueous solution. The solution was fogged to nebulize the substance and guide it by a 21 % Oxygen flux to the surface of a silicon substrate at 450 °C. Then, the sample was cleaned in a subsequent bath of ethanol and water. Finally, it was dried in nitrogen flux. To collect the nanoparticles, the sample was undergone in an ultrasonic source for 30 min and then, was centrifugated at 10,000 RPM for 10 min. On the other hand, to raise the MnFe_2O_4 nanoparticles the hydrothermal method was used following the procedure reported in our previous research work [29]. Thus, manganese chloride and an iron chloride solution were made in water. Afterward, the solutions were mixed in a proportion of 2:1 for Fe: Mn and bubbled for 30 min with a 21 % oxygen atmosphere. The solution was placed in an autoclave for performing the hydrothermal methodology. The entire system was heated to 180 °C for 4h to obtain nano-icosahedrons. The sample was recovered after synthesis and cleaned by a subsequent bath of ethanol and water. Then, it was dried into a 20 L/ min nitrogen flux.

For functionalization with SiO_2 , both kinds of nanoparticles were placed in a chemical water according to the procedure previously reported [29]. Ethanol, deionized water, and ammonia were mixed in a rate of 20:20:4 respectively. The mix was sonicated for 10 min to homogenize it. Then, the nanoparticles, Mn_3O_4 and MnFe_2O_4 , were combined with tetraethyl orthosilicate plus the mix previously obtained in separately events. The mix was held at room temperature and was stirred for 8 h to bring the Mn_3O_4 nanoparticles- SiO_2 and MnFe_2O_4 nanoparticles- SiO_2 complex, respectively.

The artificial breast tissue (ABT) was made from the reagents shown in Table 1. Thus, benzalkonium chloride, glycerin, and water were placed in a beaker and

mixed at 30 °C. Afterward, alumina powder with an average diameter of 1 μm and 0.3 μm was mixed separately with silicon carbide and agar. Both mixings were incorporated to constitute the ABT at 91 °C with constant stirring of 40 RPM/min for 3 h. Then it was cooled down in the water for 1 h and then was placed on a surface at room temperature. The dispersion of the nanoparticles was studied before and after functionalization with SiO_2 .

Table 1. List of reagents and materials with the corresponding proportion used to constitute the artificial breast tissue.

Chemical Reagent	Wt. % composition
deionized water	82.97
Glycerin	11.21
benzalkonium chloride	0.46
Agar	3
silicon carbide (17 μm)	0.53
alumina (particle size of 1 μm)	0.95
alumina (particle size of 0.3 μm)	0.88

All the samples were characterized by X-ray diffraction (XRD, Bruker D8 Eco Advance diffractometer) by using a radiation $\text{Cu } k\alpha = 1.5418 \text{ \AA}$, scanning electron microscopy (SEM, JEOL 7401F microscope) with a system for energy dispersive X-ray spectroscopy (EDS), dynamic light scattering (DLS, an Anton Paar Litesizer 500), transmission electron microscopy (TEM, JEOL ARM200F), X-ray photoelectron spectroscopy (XPS, Thermo Fisher Scientific K-alpha model) with Al $k\alpha$ monochromatic beam as beam source, and atomic force microscopy (AFM, SOL instruments NT-MDT model).

3. Results and discussion

To analyze the morphology of nanoparticles, scanning electron microscopy images were recorded. Figure 2a and b shows the comparison between the Mn_3O_4 and MnFe_2O_4 nanoparticles, where both kinds of nanoparticles are obtained with a high grade of dispersion. Transmission electron microscopy images evidence in great detail the morphology of as synthesized nanoparticles, where the Mn_3O_4 nanoparticles have a sphere-like shape (Figure 2c) and the MnFe_2O_4 nanoparticles have an icosahedron-like shape. The difference in shape could be attributed to the methodology due to Mn_3O_4 nanoparticles being synthesized

by spray pyrolysis and MnFe_2O_4 nanoparticles being obtained by hydrothermal method. Morphology could have an important effect on the application as a contrast enhancement agent in mammography images because of the surface charge linked to the staking of materials [30].

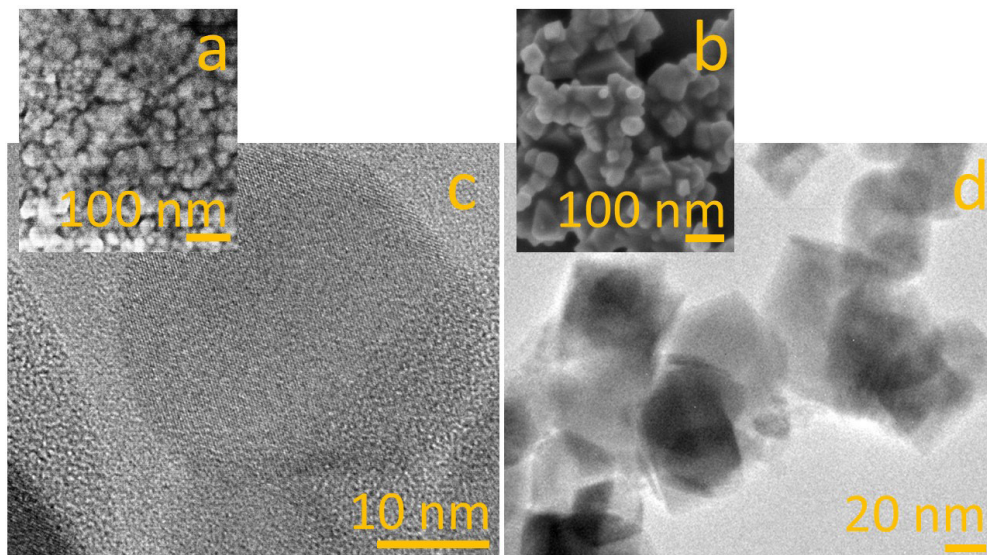


Figure 2. Scanning electron microscopy images of (a) Mn_3O_4 and (b), MnFe_2O_4 nanoparticles. Transmission electron microscopy images of (c) Mn_3O_4 and (d), MnFe_2O_4 nanoparticles.

The phase present in the samples was analyzed by X-ray diffraction. Figure 3 shows a comparison between the signal obtained from the Mn_3O_4 and MnFe_2O_4 nanoparticles. The diffraction of (011), (112), (013), (121), (004), (220), (015), (231), (033), (224), (125), (040) and (143) planes were found in good agreement for Mn_3O_4 phase [28]. The (220), (311), (400), (422), (511), and (440) planes are in good agreement for the cubic phase of MnFe_2O_4 [29]. In addition, the elemental contents were analyzed by energy dispersive X-ray spectroscopy (EDS), finding the elemental proportion according to Mn_3O_4 and MnFe_2O_4 phase, Figure 3b and 3c, respectively. Thus, the nanoparticles have a homogeneous phase according to obtained results.

Moreover, the MnFe_2O_4 nanoparticles were characterized by X-ray photoelectron spectroscopy (XPS) in four different morphologies: (i) flakes, (ii) rough-octahedrons, (iii) regular-octahedrons, and (iv) icosahedrons. Figure 4 shows the comparison between the recorded signal of the different analyzed morphologies. As can be seen in Figure 4, the proportion rate between the Fe and Mn ions is different among the samples. On the other hand, the oxygen signal (after applying

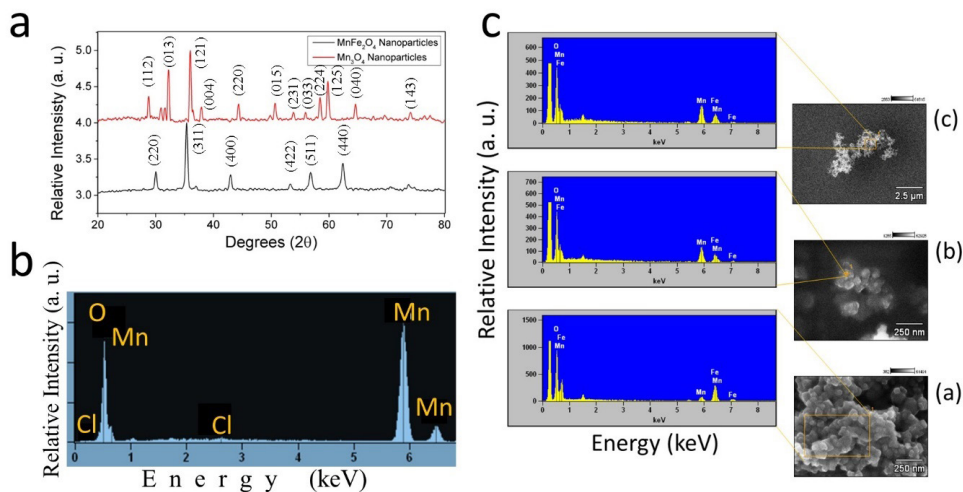


Figure 3. (a) XRD pattern comparison between Mn₃O₄ (red) and MnFe₂O₄ (black) nanoparticles. EDS spectra of (b) Mn₃O₄ nanoparticles and (c) MnFe₂O₄ nanoparticles.

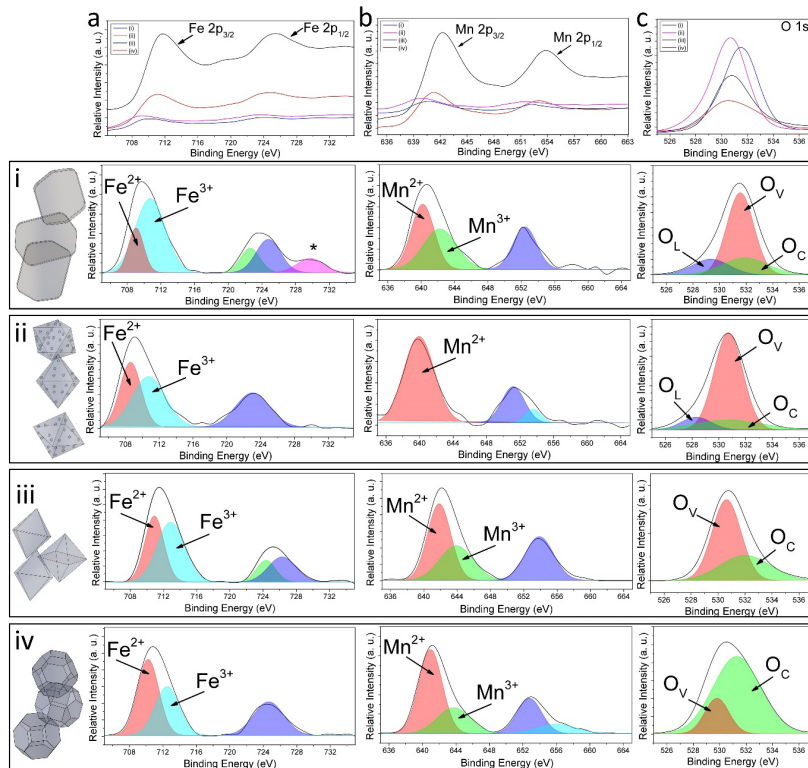


Figure 4. XPS spectra of MnFe₂O₄ nanoparticles (a) 705–735 eV, (b) 635–665 eV, and (c) 525–537 eV BE range. The gaussian fit of XPS spectra was recorded from different morphologies: (i) flakes, (ii) rough-octahedrons, (iii) regular-octahedrons, and (iv) icosahedrons. Taken from reference [29].

a Gaussian fit) unveils a strong difference in the oxygen components, and oxygen vacancy density could be the main factor linked to morphology [31, 32]. This variation in oxygen vacancies can confer an enhancement for distribution into the breast tissue and for functionalization toward drug carriers' formation.

The artificial breast tissue (ABT) is shown in Figure 5a. Figures 5b and c show a comparison between two dispersions of nanoparticles into the ABT (1 $\mu\text{g}/\text{mL}$, and 600 $\mu\text{g}/\text{mL}$). And Figures d and e show the profile of the selected region. Can be seen a clear difference in nanoparticles once they are incorporated into the ABT. The nanoparticles are well incorporated into the ABT as can be seen in the TEM image (see Figure 5f). Figures 5g and 5h show the distance between the nanoparticles according to the concentration induced by the ABT. The nanoparticles can be dispersed according to the concentration rate in the ABT, this is useful for contrast enhancement application due to dispersion guarantee a major efficiency in the material employed for this application.

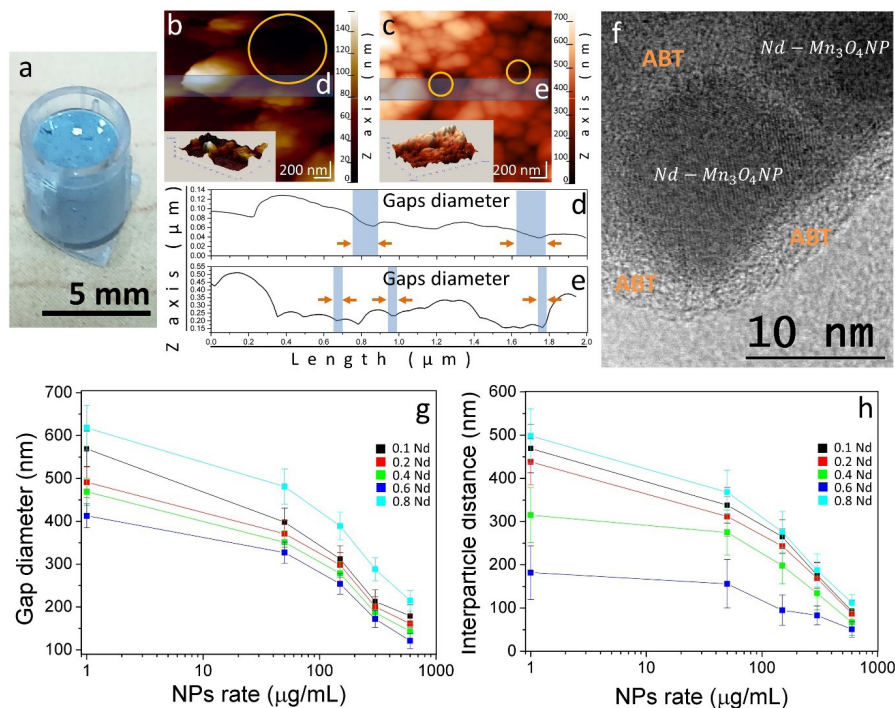


Figure 5. (a) Photograph of the ABT with nanoparticles incorporated. AFM image of Mn_3O_4 nanoparticles into ABT with a nanoparticle mass rate of (b) 1 $\mu\text{g}/\text{mL}$ and (c) 600 $\mu\text{g}/\text{mL}$. (Inserts show the 3D projection of shown area, respectively). The (d) and (e) show the roughness profile of sections depicted in (b) and (c), respectively. (f) Mn_3O_4 nanoparticles into ABT imaged by HRTEM. The relationship between the nanoparticles rate in ABT and (g) the size of the gaps, and (h) interparticle distance. Taken from reference [28].

Once the nanoparticles were functionalized, they were exposed to a breast cancer cell (BT₂₀ cell line) for 24 hours. After the time was reached, the sample was prepared for visualization in a transmission electron microscope. Figure 6 shows the nanoparticles inside the cell, this could be useful for specific targeting of breast cancer disease and specific targeting.

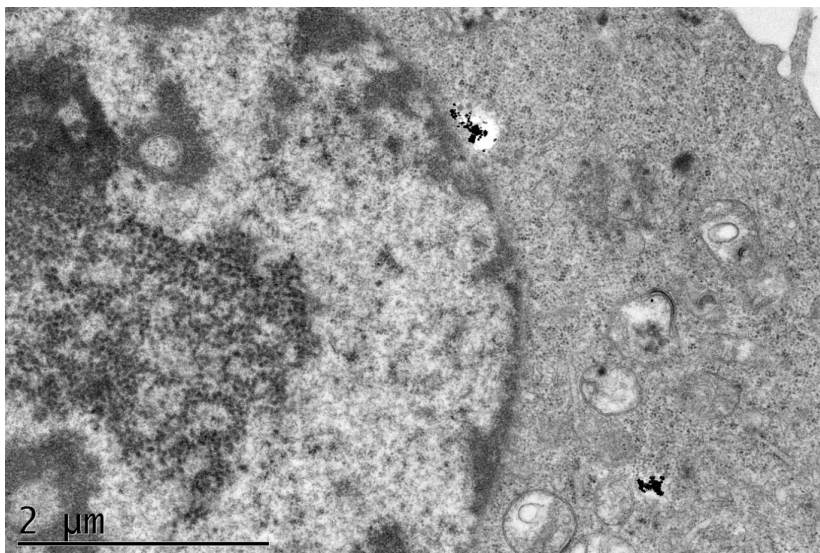


Figure 6. Transmission electron microscopy image of a breast cancer cell after 24 h of interaction with Mn₃O₄ and MnFe₂O₄ nanoparticles.

4. Conclusions

This chapter described detailed information about mammography imaging for early breast cancer detection. Although the mammography imaging technique is efficient for identifying cancer tissue, it will not always provide the best resolution of images due to the complex structure of human tissue. Therefore, the use of nanomaterials in mammography imaging will be a promising alternative as a contrast agent to detect abnormal tissue appropriately. Many studies regarding the use of different nanomaterials in mammography imaging have been found to improve the performance of imaging techniques. Despite the development of more nanomaterials in mammography imaging, the use of these nanomaterials is still associated with some limitations regarding synthesis techniques for commercialization, sensitivity, specificity, etc. To solve these challenges or limitations, highly dynamic synthesis techniques and optimization of synthesis parameters for nanomaterials should be done to get high-quality material at low-cost. Since

nanomaterials can greatly improve the survival rates for breast cancer patients, future studies should also aim at their features, their safety and efficacy profile, their potential applications, their experimental observations, etc. The Mn_3O_4 (red) and MnFe_2O_4 nanoparticles can be applied for contrast enhancement in mammography images for early breast cancer diagnosis.

Acknowledgement and Funding

The authors acknowledge the Consejo Nacional de Humanidades, Ciencia y Tecnología (CONAHCYT) for the economic support to this work through the FORDECYT-PRONACES/6005/20 project. The authors also thank the Secretaría de Investigación y Posgrado of the IPN for the partial financial support to this research.

References

1. Mukhopadhyay, S., & Chanda, B. (2000). A multiscale morphological approach to local contrast enhancement. *Signal Processing*, 80(4), 685-696.
[https://doi.org/10.1016/S0165-1684\(99\)00161-9](https://doi.org/10.1016/S0165-1684(99)00161-9)
2. Wang, L. (2017). Early diagnosis of breast cancer. *Sensors (Switzerland)*, 17(7).
<https://doi.org/10.3390/s17071572>
3. Keservani, R. K., Kesharwani, R. K., & Sharma, A. K. (2016). Nanobiomaterials involved in medical imaging technologies. In: *Nanomaterials in Medical Imaging*, 303-337. Elsevier Inc.
<https://doi.org/10.1016/B978-0-323-41736-5.00010-8>
4. Yaffe, M. J. (1990). AAPM tutorial. Physics of mammography: image recording process. *Radiographics*, 10(2), 341-363.
<https://doi.org/10.1148/radiographics.10.2.2183301>
5. Jacobs, L., & Finlayson, C. (2010). Early Diagnosis and Treatment of Cancer Series: Breast Cancer-E-Book: Expert Consult. Elsevier Health Sciences. ISBN: 9781437736106
https://books.google.com.mx/books?id=LCqw_pJc5MIC
6. Paci, E. (2002). Mammography and Beyond: Developing Technologies for Early Detection of Breast Cancer. *Breast Cancer Research*, 4(3), 123-125.
<https://doi.org/10.1186/bcr429>
7. Hansmann, M., Hackelöer, B.-J., & Staudach, A. (1986). Diagnosis of Breast Disease. *Ultrasound Diagnosis in Obstetrics and Gynecology*, 407-428.
https://doi.org/10.1007/978-3-642-70423-9_18
8. Oliver A., Freixenet, J., Martí, J., Pérez, E., Pont, J., Denton, R. R. E. *et al.* (2010). A review of automatic mass detection and segmentation in mammographic images. *Medical Image Analysis*, 14(2), 87-110.
<https://doi.org/10.1016/j.media.2009.12.005>
9. Heywang-köbrunner, S. H., Dershaw, D. D., & Schreer, I. (2001). Diagnostic breast imaging Mammography, sonography, magnetic resonance imaging, and interventional procedures. *Journal of Medical Radiation Sciences*, 62(1), 86-87.
<https://doi.org/10.1002/jmrs.90>
10. Jafari, S. H., Saadatpour, Z., Salmaninejad, A., Momeni, F., Mokhtari, M., Nahand, J. S. *et al.* (2018). Breast cancer diagnosis: Imaging techniques and biochemical markers. *Journal of Cellular Physiology*, 233(7), 5200-5213.
<https://doi.org/10.1002/jcp.26379>
11. Han, X. Xu, K. Taratula, O., & Farsad, K. (2019). Applications of nanoparticles in biomedical imaging, *Nanoscale*, 11(3), 799-819.
<https://doi.org/10.1039/C8NR07769J>

12. Zeineldin, R. (2020). Nanotechnology for cancer screening and diagnosis: from innovations to clinical applications. <https://doi.org/10.1016/B978-0-08-102983-1.00010-7>
13. Saravanakumar, K., Anbazhagan, S., Usliyanage, J. P., Naveen, K. V., Wijesinghe, U., Xiaowen, H. *et al.* (2022). A comprehensive review on immuno-nanomedicine for breast cancer therapy: Technical challenges and troubleshooting measures. *International Immunopharmacology*, 103, 108433. <https://doi.org/10.1016/j.intimp.2021.108433>
14. Silva A. D. R., Stocco, T. D., Granato, A. E. C., Harb, S. V., Afewerki, S., Bassous, N. J. *et al.* (2019). Recent Advances in Nanostructured Polymer Composites for Biomedical Applications. *Micro and Nano Technologies*, 21-52. <https://doi.org/10.1016/B978-0-12-816771-7.00002-8>
15. Shahbazi, N., Zare-Dorabei, R., & Naghib, S. M. (2021). Multifunctional nanoparticles as optical biosensing probe for breast cancer detection: A review. *Materials Science and Engineering C*, 127, 112249. <https://doi.org/10.1016/j.msec.2021.112249>
16. Chapman, S., Dobrovolskaia, M., Farahani, K., Goodwin, A., Joshi, A., Lee, H. *et al.* (2013). Nanoparticles for cancer imaging: The good, the bad, and the promise. *Nano Today*, 8(5), 454-460. <https://doi.org/10.1016/j.nantod.2013.06.001>
17. Waller, J., DeStefano, K., Chiu, B., Jang, I., Cole, Y., Agyemang, C., et al, (2022). An update on nanoparticle usage in breast cancer imaging. *Nano Select*, 3(7), 1103-1111. <https://doi.org/10.1002/nano.202100320>
18. Joudeh, N., & Linke, D. (2022). Nanoparticle classification, physicochemical properties, characterization, and applications: a comprehensive review for biologists. *Journal of Nanobiotechnology*, 20(1), 1-29. <https://doi.org/10.1186/s12951-022-01477-8>
19. Tulinski, M., & Jurczyk, M. (2017). Nanomaterials Synthesis Methods. *Metrology and Standardization of Nanotechnology*, 1, 75-98. <https://doi.org/10.1002/9783527800308.ch4>
20. Rane, A., V., Kanny, K., Abitha, V. K. & Thomas, S. (2018). Methods for Synthesis of Nanoparticles and Fabrication of Nanocomposites. In: *Synthetic of Inorganic Nanomaterials*. Elsevier Ltd. <https://doi.org/10.1016/B978-0-08-101975-7.00005-1>
21. Sreedhar, K., & Panlal, B. (2012). Enhancement of Images Using Morphological Transformations. *International Journal of Computer Science and Information Technology*, 4(1), 33-50. <https://doi.org/10.5121/ijcsit.2012.4103>

22. Hofvind, S., Iversen, B. F., Eriksen, L., Styr, B. M. Kjellevold, K., & Kurz, K. D. (2011). Mammographic morphology and distribution of calcifications in ductal carcinoma in situ diagnosed in organized screening. *Acta Radiologica*, 52(5), 481-487.
<https://doi.org/10.1258/ar.2011.100357>
23. Reljin, B. Milošević, Z. Stojić, T., & Reljin, I. (2009). Computer aided system for segmentation and visualization of microcalcifications in digital mammograms. *Folia Histochemica et Cytobiologica*, 47(3), 525-532.
<https://doi.org/10.2478/v10042-009-0076-1>
24. Kimori, Y. (2013). Morphological image processing for quantitative shape analysis of biomedical structures: Effective contrast enhancement. *Journal of Synchrotron Radiation*, 20(6), 848-853.
<https://doi.org/10.1107/S0909049513020761>
25. Kimori, Y. (2011). Mathematical morphology-based approach to the enhancement of morphological features in medical images. *Journal of Clinical Bioinformatics*, 1(1), 1-10.
<https://doi.org/10.1186/2043-9113-1-33>
26. Hassanpour, H., Samadiani, N., & Mahdi Salehi, S. M. (2015). Using morphological transforms to enhance the contrast of medical images. *Egyptian Journal of Radiology and Nuclear Medicine*, 46(2), 481-489.
<https://doi.org/10.1016/j.ejrn.2015.01.004>
27. Gaona-Esquivel, A., Hernandez-M, D. M., Hernández-Rodríguez, Y. M., & Cigarroa-Mayorga, O. E. (2022). The role of Nd as a dopant in Mn₃O₄NPs on the heat induction of artificial breast tissue due to the irradiation of microwaves. *Materials Chemistry and Physics*, 292, 126822.
<https://doi.org/10.1016/j.matchemphys.2022.126822>
28. Gaona-Esquivel, A., Hernández-M, D., Sánchez-Trujillo, P. J., Cigarroa-Mayorga, O. E., & Meléndez-Lira, M. (2020). Hyperthermia Effect on Phantom of Breast Carcinoma Tissue Induced by Mn₃O₄ Nanoparticles Synthesized by One-Step Spray Pyrolysis Method. *Key Engineering Materials*, 853, 56-60.
<https://doi.org/10.4028/www.scientific.net/KEM.853.56>
29. Cigarroa-Mayorga, O. E. (2021). Tuning the size stability of MnFe₂O₄ nanoparticles: Controlling the morphology and tailoring of surface properties under the hydrothermal synthesis for functionalization with myricetin. *Ceramics International*, 47(22), 32397-32406.
<https://doi.org/10.1016/j.ceramint.2021.08.139>
30. Palomino, J., Varshney, D., Weiner, B. R., & Morell, G. (2015). Study of the structural changes undergone by hybrid nanostructured Si-CNTs employed as an anode material in a rechargeable lithium-ion battery. *Journal of Physical Chemistry C*, 119, 21125-21134.
<https://doi.org/10.1021/acs.jpcc.5b01178>

31. Raj, A.M.E., Victoria, S.G., Jothy, V.B., Ravidhas, C., Wollschläger, J., Suendorf, M. *et al.* (2010). XRD and XPS characterization of mixed valence Mn_3O_4 hausmannite thin films prepared by chemical spray pyrolysis technique. *Applied Surface Science*, 256(9), 2920-2926.
<https://doi.org/10.1016/j.apsusc.2009.11.051>
32. He, M., Zeng, Y., Zhou, F., Kong, G., Lu, Y., Chen, W. *et al.* (2020). $MnFe_2O_4$ nanoparticles anchored on the surface of MgAl-layered double hydroxide nanoplates for stable magnetorheological fluids *Journal of Molecular Liquids*, 319, 114098.
<https://doi.org/10.1016/j.molliq.2020.114098>